

Adaptive Crystal Structures: CuAu and NiPt

M. Sanati, L. G. Wang, and Alex Zunger

National Renewable Energy Laboratory, Golden, Colorado 80401

(Received 12 June 2002; published 31 January 2003)

We discover that Au-rich $\text{Cu}_{1-x}\text{Au}_x$ and Pt-rich $\text{Ni}_{1-x}\text{Pt}_x$ contain a composition range in which there is a quasicontinuum of stable, ordered “adaptive structures” made of (001) repeat units of simple structural motifs. This is found by searching $\sim 3 \times 10^6$ different fcc configurations whose energies are parametrized via a “cluster expansion” of first-principles-calculated total energies of just a few structures. This structural adaptivity is explained in terms of an anisotropic, long-range strain energy.

DOI: 10.1103/PhysRevLett.90.045502

PACS numbers: 61.50.-f, 61.43.-j, 61.66.-f

One of the usual canons of solid state chemistry and metallurgy is that at low temperatures the equilibrium phase diagram of ordering alloys shows only a limited number of stable ordered phases (“line compounds”) [1–3]. These line compounds appear at simple, Daltonian stoichiometric ratios and have fairly small unit cells. This fundamental paradigm led to the traditional description of ordered “ground state structures” in terms of Ising Hamiltonian [4–8] with fairly short-range interatomic interactions. For example, if binary fcc $A_{1-x}B_x$ compounds are described via an Ising Hamiltonian with nearest neighbor interatomic interactions of arbitrary magnitude [6–8], a complete search of all possible ground states reveals a total of five possible zero-temperature structures, appearing at compositions $x = 0, 0.25, 0.5, 0.75,$ and 1 . However, in 1973, Anderson [9] noted experimentally the existence of a group of crystalline materials where, “within certain composition limits, every possible composition can attain a unique, fully ordered structure without defects.” Furthermore, such “infinitely adaptive structures” had a multiplicity of discrete higher energy, fully ordered structures which were separated energetically by only a small amount, for any one composition. An example of the then recognized [9] infinitely adaptive structures included phases related to low-temperature Ta_2O_5 , crystallographic “shear phases” of TiO_2 , ReO_3 -type, MoO_3 and $\alpha\text{-PbO}_2$ structures, and the “microphases” of CeCd . In 1978, Kittel suggested [10] that long-range repulsive interactions can account for such infinite adaptivity [11]. However, even modern parametrizations of alloy Ising Hamiltonians from experimental data [12] or first-principles calculations [13,14] have been generally restricted to rather short-range interactions and thus could not reveal if a given alloy system has adaptive structures or not. We have previously developed a generalized Ising Hamiltonian (“mixed basis cluster expansion”) [15] in which the range of interactions and their types (pairs, triangle, tetrahedra, ...) are decided via first-principles total-energy calculations on a set of configurations of various arrangements $A_p B_q$ of A and B atoms on a lattice. The expansion is given in terms of chemical (pair and multiatom) interactions, as well as long-range,

repulsive strain-driven elastic pair interactions, resulting from the forced coherence of the size-mismatched A and B planes along arbitrary crystallographic directions. The interaction energies are determined by the requirement that this cluster expansion reproduce the accurate configurational energies obtained by first-principles total-energy calculations. This condition produces for many transition metal alloys fairly long-range chemical interactions (~ 20 – 40 different pairs; 5 – 10 multibody terms), in addition to the formally infinite-range elastic interactions. We show here that a $T = 0$ ground state search of such a first-principles configurational Hamiltonian reveals for NiPt and CuAu a composition range, exclusively on the heavy-metal-rich side, exhibiting a dense, quasicontinuum of stable ground states, each having low-energy excited configurations. We identify the structural motifs in such “adaptive structures,” explain its stability. Although various long-period structures based on CuAu were previously identified [1] as *entropy-stabilized finite temperature structures* (e.g., CuAu-II), the $T = 0$ infinitely adaptive ground state structures are unsuspected [16,17].

Within the cluster expansion method [15] one selects an underlying parent lattice (e.g., fcc) and defines a configuration σ by specifying the occupations of each of the N lattice sites per cell by an A (spin index $S_i = -1$) or a B atom (spin index $S_i = 1$). The excess energy (with respect to equivalent amounts of solid A and B) of any spin configuration σ , at its locally atomically relaxed minimum energy state, is then expanded as

$$\Delta H_{\text{CE}}(\sigma) = \sum_{\mathbf{k}} J_{\text{pair}}(\mathbf{k}) |S(\mathbf{k}, \sigma)|^2 + \sum_f^{\text{MB}} D_f J_f \bar{\Pi}_f(\sigma) + \sum_{\mathbf{k}} \frac{\Delta E_{\text{cs}}^{\text{eq}}(x, \hat{\mathbf{k}})}{4x(1-x)} |S(\mathbf{k}, \sigma)|^2 F(\mathbf{k}). \quad (1)$$

The first summation includes all pair figures corresponding to pair interactions with arbitrary separation. $J_{\text{pair}}(\mathbf{k})$ is the Fourier transform of the pair interaction energies and $S(\mathbf{k}, \sigma)$ is the structure factor of configuration σ . The second sum includes only nonpair figures. Here J_f is the real-space effective many-body interactions of figure f ,

D_f stands for the number of equivalent clusters per lattice site, and $\overline{\Pi}_f(\sigma)$ are spin products. The third summation represents atomic size-mismatch effects and involves the “constituent strain energy” $\Delta E_{cs}^{eq}(x, \hat{k})$ necessary to maintain coherency between A and B along an interface with orientation \hat{k} , and $F(\mathbf{k})$ is the attenuation function for short wavelengths. This third term gives rise to a long-range interaction in real space and includes a nonanalytic, $k \rightarrow 0$ behavior.

All quantities of Eq. (1) are determined from first-principles total-energy calculations [15]. $\Delta E_{cs}^{eq}(x, \hat{k})$ is obtained from a set of LDA (local density approximation) calculations on biaxially strained A and B solids. We determined $\{J_{\text{pair}}(\mathbf{k})\}$ and $\{J_f\}$ by fitting $\Delta H_{CE}(\sigma_{\text{ord}})$ to a set $\{\sigma_{\text{ord}}\}$ of LDA-calculated formation energies $\Delta H_{\text{LDA}}(\sigma_{\text{ord}})$ of ordered (not necessarily ground states) $A_p B_q$ compounds. The formation enthalpies, $\Delta H_{\text{LDA}}(\sigma_{\text{ord}})$, were calculated using density functional theory, as implemented in the ultrasoft pseudopotential (for NiPt) and projector augmented wave (for CuAu) representations, using the VASP code [18]. For each structure, we relax both the cell-external lattice vectors and the atomic cell-internal degrees of freedom to obtain minimum energies. To assume the best cancellation of systematic errors in $\Delta H_{\text{LDA}}(A_p B_q) = E(A_p B_q) - \frac{p}{p+q}E(A) - \frac{q}{p+q}E(B)$, we use the *same* high numerical precision in the total energies of all three terms on the right-hand side, including the use of geometrically equivalent k points, identical integration meshes, and basis sets. ΔH_{LDA} is stable to within 2 meV/atom, and the precision of ΔH_{CE} relative to the directly calculated ΔH_{LDA} is 1 meV/atom. We verified [19] that using different exchange-correlation functionals [the generalized gradient approximation (GGA)] and spin polarization does not alter our conclusions. The interactions in Eq. (1) were obtained by first eliminating from the fit several of the ordered structures $\{\sigma_{\text{ord}}\}$ and choosing the interactions that result in an accurate fit to the structures retained as well as accurate predictions for the eliminated structure. The process is repeated using different sets of eliminated structures to ensure a set of interactions that work well generally. In the case of NiPt, a very robust fit was obtained with 35 input structures, requiring 20 pairs and 10 three-body and four-body interactions. For the CuAu system we used 33 input structures and needed 26 pairs and 5 three-body and four-body interactions.

We subject our cluster-expanded Hamiltonian to a “direct enumeration ground state search” [20] in which every fcc configuration that can be constructed from a unit cell with N sites is examined. We use $N \leq 20$, delivering up to 3×10^6 possible structures. The ground states of $\text{Cu}_{1-x}\text{Au}_x$ and $\text{Ni}_{1-x}\text{Pt}_x$ are shown in Fig. 1 as solid circles connected by a convex-hull line. These circles correspond to structures that are the absolute stable forms with respect to other structures at the same composition, and with respect to phase separation into structures of neighboring compositions. In some cases we validate the

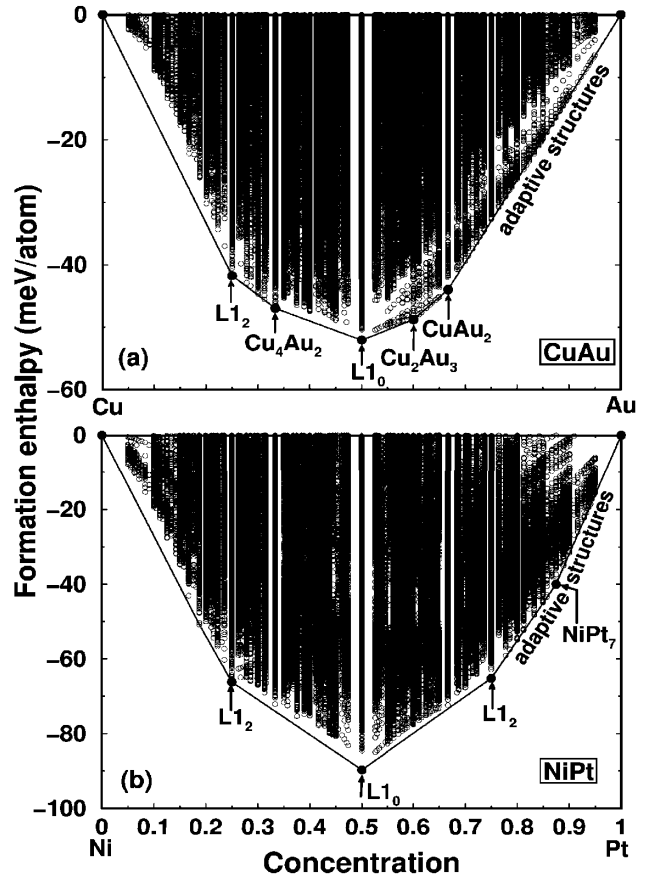


FIG. 1. Results of a ground state search for unit cells containing up to 20 sites for (a) Cu-Au and (b) Ni-Pt systems. Arrows denote the ground states identified out of 3 039 674 configurations searched.

results of a direct enumeration search by performing Monte Carlo simulated annealing, with larger cells containing $20 \times 20 \times 20$ primitive cells ($N = 8000$ sites), finding the same ground states.

Discrete structures.—Examination of the ground state diagram (Fig. 1) reveals that in the composition range rich in the light element (Ni in NiPt and Cu in CuAu) there are but a few, discrete ground states, separated by a considerable “energy gap” from the higher energy excited configurations. In this range we confirm the known [3] Cu_3Au (L_{1_2}) and Ni_3Pt (L_{1_2}) ground state structures. We further *predict* [19] a new, discrete orthorhombic structure Cu_4Au_2 with lattice constants $a = 3.727 \text{ \AA}$, $b = 3.702 \text{ \AA}$, and $c = 11.238 \text{ \AA}$ as well as tetragonal structures for Cu_2Au_3 , CuAu_2 , and NiPt_7 with lattice constants $[a(\text{\AA}), c(\text{\AA})] = (3.968, 18.761)$, $(3.948, 11.422)$, $(3.863, 15.464)$, respectively. The crystal structures of these new ground states are shown in Fig. 2. We calculate the order-disorder transition temperatures for the new ground states using the Monte Carlo simulation technique [16,17] and find that all transitions are first order, involving discontinuities in the energy and specific heat [16]. The latter is used to determine the order-disorder transition temperatures for Cu_3Au (L_{1_2}), Cu_4Au_2 , CuAu (L_{1_0}),

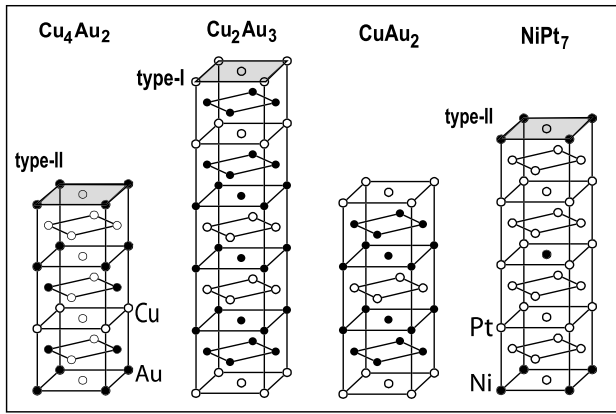


FIG. 2. The crystal structures of the ground states predicted for Cu-Au and Ni-Pt. These structures are constructed by (001) stacking of two different types (I and II) of planes.

Cu_2Au_3 , CuAu_2 , NiPt_7 as 412, 516, 575, 587, 597, and 371 K, respectively.

Adaptive structures.—Figure 1 shows that in the heavy metal rich compositions there is a (quasi)continuum [21] of ordered structures, separated at each composition by only a vanishingly small energy difference from the next excited configurations. Examining the crystal structures at those compositions, we find that they are all made from (001) stacking of two simple fcc lattice planes, denoted in Fig. 2 as type-I and type-II planes. For $\text{Cu}_{1-x}\text{Au}_x$, the adaptive ground states are superstructures made of alternating pure-Cu and pure-Au planes of type I, where each Cu monolayer is always separated from the next by a minimum of one Au monolayer $(I_{\text{Cu}})_1/(I_{\text{Au}})_n/(I_{\text{Cu}})_1$. No (001) plane includes both Cu and Au atoms. These adaptive structures can be viewed, alternatively, as made of equiatomic CuAu $L1_0$ structure [alternate monolayer superlattice of Cu and Au planes along (001) direction], layered by a few monolayers of Au. Figure 2 illustrates a few examples, e.g., $(L1_0)_1/(Au)_1/(L1_0)_2/(Au)_1$ for Cu_2Au_3 . (These structures may also be viewed as $L1_0$ with antiphase boundaries.) For $\text{Ni}_{1-x}\text{Pt}_x$, the adaptive structures are superstructures of the basic type-II plane with pure Pt, i.e., $(II)_1/(Pt)_m/(II)_1/(Pt)_n$. Figure 2 illustrates the new NiPt_7 ground state structure with $m = n = 3$. These one-dimensional-like superstructures are reminiscent of “Devil staircase” polytypes [22].

To understand quantitatively our finding we break the excess total energy into a “chemical” piece E_{chem} [first two terms in Eq. (1)] and a strain energy piece E_{strain} [last term in Eq. (1)]. Figure 3(a) shows the decomposition of the $\text{Cu}_{1-x}\text{Au}_x$ excess total energies of structures at and near the ground state line into E_{chem} and E_{cs} . We see that the chemical energy is roughly symmetric about $x = 0.5$; however, the strain energy E_{cs} is significantly lower at the Au-rich than at the Cu-rich side. This reflects that under expansion, Cu and Ni become rather soft in the (001) direction, since these elemental solids have a *low-lying* bcc “excited state” connected to the fcc phase via (001)

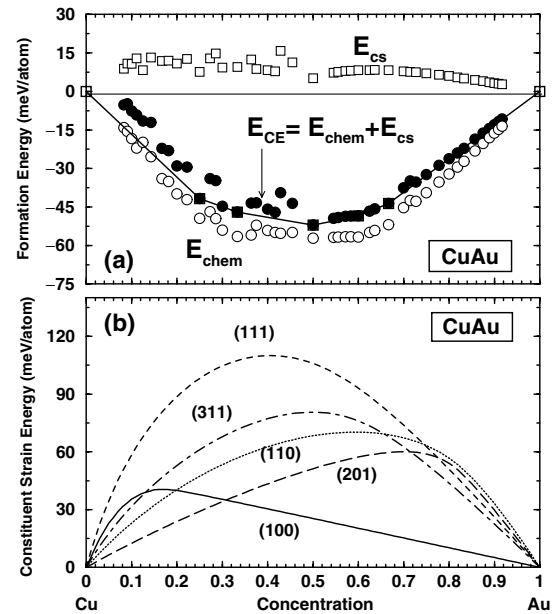


FIG. 3. (a) Separation of the cluster expansion energy E_{CE} of Cu-Au alloys into chemical E_{chem} and strain energy E_{cs} parts. (b) The calculated constituent strain energies for Cu-Au along several principle directions.

(Bain-like) expansion [23]. Thus, the constituent-strain energy in Fig. 3(b) is soft for (001) expansion (i.e., Au-rich alloys). No such softening exists for *compression* of Au or Pt (i.e., Cu- or Ni-rich alloys). This analysis shows the following:

(i) For the *Cu-rich* alloys, the choice of ground state structures is based primarily on the optimization of the *chemical* energy part. In this composition range the strain energy is big (corresponding to the insertion of large Au atoms/planes into the smaller size Cu lattice), but strain does not offer any particular structural selectivity, as different orientations of Cu/Au planes result in similar constituent-strain energies [see Fig. 3(b) for $x \leq 0.1$]. Yet, the chemical energy prefers Cu-Au bonds over the average of Cu-Cu and Au-Au (thus, $E_{\text{chem}} < 0$). Consequently, the ground state structures Cu_3Au ($L1_2$) and Cu_4Au_2 are built from type-II lattice planes (Fig. 2) containing both Cu and Au atoms. Only these two structures emerge in this composition range as having exceptionally stable chemical energy, while all others are well above the tie-line connecting pure Cu with Cu_3Au ($L1_2$). This is because the strain energy is large in Cu-rich alloys, pushing the energies of all the structures above the tie-line.

(ii) For the *Au-rich* composition range, we find that the choice of ground state structures is based primarily on the optimization of the *strain energy* part. Here [Fig. 3(a)] the strain energy is smaller (corresponding to the insertion of small Cu atom/planes into the bigger size Au lattice), so the energies are not pushed up as far as in the Cu-rich case, and many structures remain on (or near) the tie-line. However, as noted above, the strain along

the (001) direction is particularly soft [Fig. 3(b)], thus offering a clear structural selectivity. On the other hand, the chemical energy is less selective here: The calculated Cu-Au bond strength of 179 kJ/mol (cohesive energy per bond obtained by adding the theoretical compound heat of formation to the experimental heat of atomization of the elemental solids [24]) is rather similar to the Cu-Cu or Au-Au bond strength (168 kJ/mol and 184 kJ/mol for Cu-Cu and Au-Au, respectively). Therefore, there is no large chemical penalty for forming planes of pure Cu-Cu or pure Au-Au bonds without cross Cu-Au bonds, yet there is a substantial gain in strain energy [particularly for (001) stacking] in doing so. Thus, the ground state structures are based on (001) stacking of type-I planes (Fig. 2), consisting of pure Cu and pure Au. The reason that the stable repeat unit consists of a subunit of $(I_{\text{Cu}})_1(I_{\text{Au}})_1 \equiv L1_0$ layered with n monolayers of Au is that this particular structural motif offers exceptionally low (001) strain: the $L1_0$ structure of CuAu has tetragonal symmetry, permitting its (001) tetragonal c/a ratio to deviate from 1. Our calculations show that $c/a = 0.915$. This (001) shrinkage is accompanied (via the volume conservation principle) by a significant expansion of the in-plane lattice constant, beyond the 50%-50% (Vegard) value. This in-plane expansion gives $a_{\text{in-plane}}$ that is nearly (within 3.2%) lattice matched with pure fcc Au. Thus, (001) stacking of Au on $L1_0$ CuAu costs only little strain energy. This suggests that the Au-rich alloy will have particularly low interfacial energies, with potential implications on microstructural morphology.

In the NiPt system one can draw a similar conclusion about the stacking of the planes along the (001) direction, since the strain energy of NiPt is very similar to that in CuAu; i.e., strain energy along the (001) direction at the Pt-rich region is much softer with respect to the other high symmetric directions. Therefore, as in the CuAu system one expects to see adaptive structures with (001) orientation at the Pt-rich region. However, contrary to the CuAu system, the Ni-Pt bond strength (calculated at 252 kJ/mol) is stronger than the Ni-Ni bond (214 kJ/mol [24]), which means the pure Ni atomic planes are unfavorable. But the pure Pt atomic planes are energetically favorable because of the strong Pt-Pt bonds (282 kJ/mol [24]). Consequently, adaptive structures at the Pt-rich side prefer to have mixed Ni-Pt (001) planes layered with pure Pt planes, but without pure Ni planes.

We conclude that fcc adaptive structures of the sort discovered here must contain an fcc element whose bcc energy is not too high above fcc (Cu, Ni), and a larger element (Pt, Au) that acts to expand the smaller element into the regime of its transition to bcc, thus creating asymmetric (001) strain softness. We call for experimental testing of this novel concept of phase ordering.

This work is supported by the U.S. Department of Energy, SC-BES-OER Grant No. DE-AC36-98-GO10337. We thank V. Ozoliņš and C. Wolverton for discussions.

- [1] D. de Fontaine and J. Kulik, *Acta Metall. Mater.* **33**, 145 (1985).
- [2] W.B. Pearson, *The Crystal Chemistry and Physics of Metals and Alloys* (Wiley Interscience, New York, 1972).
- [3] R. Hultgren, P.D. Desai, D.T. Hawkins, M. Gleiser, and K. Kelley, *Selected Values of the Thermodynamic Properties of Binary Alloys* (American Society for Metals, Metals Park, OH, 1973).
- [4] D.M. Berley, in *Phase Transition and Critical Phenomena*, edited by C. Domb and M.S. Green (Academic Press, London, 1972), p. 329.
- [5] D.F. Styer, M.K. Phani, and J.L. Lebowitz, *Phys. Rev. B* **34**, 3361 (1986).
- [6] K. Binder, *Phys. Rev. Lett.* **45**, 811 (1980).
- [7] J. Kanamori and Y. Takehashi, *J. Phys. (Paris), Colloq.* **38**, C7-274 (1977).
- [8] F. Ducastelle, *Order and Phase Stability in Alloys* (North-Holland, Amsterdam, 1991), Chap. 3.
- [9] J.S. Anderson, *J. Chem. Soc. Dalton Trans.* **10**, 1107 (1973).
- [10] C. Kittel, *Solid State Commun.* **25**, 519 (1978).
- [11] An infinite set of ground states is also predicted near $x = 0.5$ on a honeycomb 2D lattice with three nearest neighbors pair interactions that satisfy certain inequalities. See J. Kanamori, *J. Phys. Soc. Jpn.* **53**, 250 (1984).
- [12] C. Sigli and J.M. Sanchez, *Acta Metall.* **33**, 1097 (1985).
- [13] J.W.D. Connolly and A.R. Williams, *Phys. Rev. B* **27**, 5169 (1983).
- [14] J. Hafner, *From Hamiltonian to Phase Diagram*, *Solid State Science Vol. 70* (Springer-Verlag, Berlin, 1987).
- [15] A. Zunger, in *Statics and Dynamics of Alloy Phase Transformation*, edited by P.E.A. Turchi and A. Gonis (Plenum, New York, 1994); A. Zunger, L.G. Wang, G. Hart, and M. Sanati, *Modell. Simul. Mater. Sci. Eng.* **10**, 685 (2002); D.B. Laks, L.G. Ferreira, S. Froyen, and A. Zunger, *Phys. Rev. B* **46**, 12587 (1992).
- [16] V. Ozoliņš, C. Wolverton, and A. Zunger, *Phys. Rev. B* **57**, 6427 (1998).
- [17] C. Wolverton, V. Ozoliņš, and A. Zunger, *Phys. Rev. B* **57**, 4332 (1998).
- [18] G. Kresse and J. Furthmüller, *Phys. Rev. B* **54**, 11169 (1996).
- [19] First-principles calculations within GGA (LDA) give for $\text{Cu}_3\text{Au}(L1_2)$, Cu_4Au_2 , $\text{CuAu}(L1_0)$, Cu_2Au_3 , and CuAu_2 ; -43.3 (-40.9), -50.6 (-47.5), -55.1 (-52.8), -51.5 (-48.9), and -46.3 (-43.2) meV/atom, respectively. Ground states in LDA are still ground states in GGA. Furthermore, spin-polarized calculations for Ni and the Ni-Pt system showed that NiPt_7 , $\text{NiPt}(L1_0)$, and $\text{Ni}_3\text{Pt}(L1_2)$ are still ground states.
- [20] L.G. Ferreira, S.-H. Wei, and A. Zunger, *Int. J. Supercomput. Appl.* **5**, 34 (1991).
- [21] Our computational error of ~ 1 meV could add (remove) some structures from the tie-line, but the existence of a quasicontinuum is robust.
- [22] M. Fisher and W. Selke, *Phys. Rev. Lett.* **44**, 1502 (1980).
- [23] V. Ozoliņš, C. Wolverton, and A. Zunger, *Phys. Rev. B* **57**, 4816 (1998).
- [24] C. Kittel, *Introduction to Solid State Physics* (John Wiley & Sons, Inc., New York, Chichester, Brisbane, Toronto, Singapore, 1986), 6th ed.